

Quantum Approximation Optimization Algorithm for the trellis based Viterbi decoding of classical error correcting codes

Mainak Bhattacharyya¹ and Ankur Raina²

¹Department of Physics, National Institute of Technology Jamshedpur, India

²Department of Electrical Engineering and Computer Science, Indian Institute of Science Education and Research Bhopal, India

We construct a quantum-classical Viterbi decoder for the classical error-correcting codes. Viterbi decoding is a trellis-based procedure for maximum likelihood decoding of classical error-correcting codes. In this article, we show that any number of paths with the minimum Hamming distance with respect to the received erroneous vector present in the trellis can be found using the quantum approximate optimization algorithm. We construct a generalized method to map the Viterbi decoding problem into a parameterized quantum circuit for any classical linear block codes. We propose a uniform parameter optimization strategy to optimize the parameterized quantum circuit. We observe that the proposed method is efficient for generating low-depth trainable parameterized quantum circuits. This renders the hybrid decoder more efficient than previous attempts at making quantum Viterbi algorithm. We show that using uniform parameter optimization, we obtain parameters more efficiently for the parameterized quantum circuit than many previous attempts made through random sampling and fixing the parameters.

1 Introduction

Classical error correcting codes are designed to tackle the noise occurring in communication channels and data storage channels. Encoding of these codes corresponds to the introduction of redundancy into the information bits. The resultant bits form the codeword. But a good code must have an efficient decoding technique alongside the encoding process. After receiving an erroneous signal/vector from the communication channel, the decoder tries to find the most likely transmitted codeword. But often the decoding problem is hard. A standard but classically exhaustive decoding process is the maximum likelihood (ML) decoding. Convolution codes and linear block codes are examples of classical error correcting codes that can be decoded using ML decoding. Given any codeword, the ML decoding calculates the probabilities of receiving a particular erroneous vector. The codeword having the maximum probability is decoded as the best candidate in the codespace. The searching process in the codespace using the maximum likelihood approach is NP-hard for a general class of linear codes. ML decoding can be cast as a form of syndrome decoding, where

Mainak Bhattacharyya: 2021pgphph09@nitjsr.ac.in

Ankur Raina: ankur@iiserb.ac.in

from the received erroneous vector and the parity check matrix of the linear block code, the syndrome corresponding to the error is determined. The search is then carried out for a member of the codespace which has the given syndrome. This problem is proven to be NP-complete by Berlekamp *et al.* in 1978 [3]. This suggests there exists no algorithm to solve the problem in polynomial time in the number of bits in the codeword. In 1990 Bruck and Naor showed that in general the knowledge of the code does not improve the decoding complexity [7]. Even preprocessing for desired order does not guarantee an efficient decoder. This suggests that there are some linear block codes which can not be decoded efficiently. ML decoding with preprocessing refers to determining the availability of vectors having Hamming weight less than a given non-negative value.

Codewords of linear block codes in a systematic form represent information bits followed by redundant bits. Thus, the codeword forms a block-like structure. Convolution codes do not have a block-like representation. The output codeword depends on the current input and the memory elements of the encoder. The encoder takes stream of input bits and produce output codeword and update the state of the encoder. For the decoding of convolution codes Viterbi algorithm [23] introduced by Viterbi is based on the maximum a posteriori probability calculations. The general problem is, given a erroneous vector determine the codeword having the maximum probability. A trellis based approach of Viterbi decoding was thoroughly discussed by Forney [12]. Any path traversing through the trellis is a valid codeword. The trellis decoding problem is also a maximum likelihood decoding. But here, the maximum a posteriori probability of a codeword, given the received vector is being searched using a path metric. After receiving the erroneous vector, the decoded codeword corresponds to the shortest path through the trellis. The path metric corresponds to the total Hamming distance of the partial branches of the trellis and the corresponding bits of the received erroneous vector. In a paper by Bahl *et al.* [2] trellis construction for linear block codes was introduced. Thus any trellis based decoding might as well be applied to the linear block codes.

During 1992-1997, quantum algorithms showed the promise to provide speedup over the corresponding classical counterparts of certain problems [9] [4] [22]. One of them introduced by LK Grover in 1996 [14] is considered to be one of the prime quantum algorithms showing outstanding speed up compared to the classical algorithms having worst case complexity. Grover's algorithm uses oracle based approach to search for an item in a disordered data set with quadratic speedup. Jung *et al.* used the inspiration from Grover's search to achieve a quadratic speed up over classical ML decoding [16]. Quadratic speed up is also achieved for the NP-complete syndrome decoding problem using a modified Grover's search algorithm [5]. The authors argued that the Grover inspired algorithm significantly reduces the time complexity of decoding than the classically exponential one. The problem of finding the path with minimum path metric can be addressed by a quantum minima finding algorithm given by Durr-Hoyer [10]. This can bring quadratic speed up in the search process. But the quantum circuits promised by the above algorithms are vulnerable to errors in the NISQ devices [20]. Our approach towards the trellis based decoding is based on the quantum approximation optimization algorithm (QAOA). We give a Quantum-classical hybrid approach for the Viterbi decoder, inspired from the QAOA introduced by Farhi *et al.* in 2014 [11]. Here the parameterized quantum circuit (PQC) evaluate the cost function with better time complexity than the classical cost function evaluation methods. Classically the complexity rises exponentially with increasing number of bits. But the success of finding a good approximate solution depends on finding a set of good parameters for the PQC. But choosing good parameters also depends on properly choosing the initial parameters and cost functions. Otherwise due to the presence of flat optimization

landscape it is often very hard to find the global minima. In their work, Bittel and Kliche showed that the classical optimization of the parameterized quantum circuits are NP hard [6]. In this regard we suggest a simple uniform parameter optimization (UPO) technique to determine good parameters for the QAOA circuit. We observe that our approach towards optimization is better than both the random initialization method and fixed parameter optimization (FPO) strategy suggested in [17]. A quantum algorithm for Viterbi decoding of classical convolution codes is proposed by Grice and Meyer [13]. They used quantum amplitude amplification technique followed by an encoding of path probabilities into the phases to increase the probability of the decoded state. But the algorithm requires quadratic iterations of phase marking and state amplitude amplification and thus renders inefficient. Variational approach is thus an efficient alternative for the trellis based Viterbi decoding. The quantum approximation optimization problem which primarily focuses to solve the combinatorial optimization problems, is used to find an approximate solution to the problems. Due to its efficiency for even lower depths, it is thought to be the best candidate for NISQ devices. We would like to point out beforehand that the depth of the parameterized quantum circuit still depends on the structure of the code itself, which includes the minimum Hamming distance and the number of bits in the codeword. Thus a generalized implementation may need error correcting codes as well. But QAOA still has better efficiency than the iterative quantum phase estimation. We show that the depth implicitly depends on the minimum Hamming distance or the structure of the code. This is arguably better than the quadratic depth dependence on fanout and the number of bits used to represent the state, suggested by Grice and Meyer.

The paper is organized as follows. We briefly discuss the trellis-based Viterbi decoding for classical linear block codes in Section 2. We also briefly mention the workflow of QAOA in Section 3. Then we formally introduce the quantum-classical (hybrid) Viterbi decoder by encoding the Viterbi decoding problem for the QAOA in Section 4. We show a general method for constructing the mixer Hamiltonian, which depends on the minimum Hamming distance of the code in Theorem 1. We propose an uniform parameter optimization (UPO) strategy in Section 5 and analyse the performance of the strategy for linear block codes. Finally we extend the application of the hybrid Viterbi decoder for the classical convolution codes in Section 6. We do all the simulations of the algorithm using qasm simulator of IBM Quantum Experience.

List of notations

Here we describe certain symbols we use frequently throughout the paper.

$0_{1 \times n}$ Row vector of n zeros.

α Approximation ratio with respect to the minimum value of cost function.

$|\psi_{in}\rangle$ Initial guess of the solution state, and must be a member of the codespace.

\mathbf{G} Generator matrix of a linear block code.

\mathbf{H} Parity check matrix of a linear block code.

\mathcal{C} Codespace

H Hadamard gate.

X Pauli-X gate.

Z	Pauli-Z gate.
c	Codeword belonging to \mathcal{C} .
c_j	j^{th} bit of a codeword.
$d(x_j, x_k)$	Hamming distance between two states x_j and x_k .
d	minimum Hamming distance of the code.
$f(x)$	Cost function dependent on codeword x .
f	Array for storing the expectation of cost function value at each sampling.
H_f	Cost function Hamiltonian.
H_m	Mixer Hamiltonian.
k	Number of bits in the information/ message.
m_i	Number of occurrence of i^{th} state upon measuring the PQC.
n	Number of bits in the codeword.
p	Number of unitary layers applied in the parameterized quantum circuit in QAOA.
p_1, p_2	Optimized Parameters.
q	Number of samples for opting out best parameters.
r	received erroneous vector.
t_β, t_γ	Optimized parameters for each sampling instances.
U_f	Cost unitary
U_g	Unitary for creating uniform superposition of all valid trellis paths.
U_m	Mixer/ Mixer unitary
$w_H(c)$	Hamming weight of the codeword.

2 Viterbi decoding of classical codes

Viterbi decoding is a maximum likelihood technique for decoding the codeword after receiving the erroneous vector. The decoder is essentially a trellis-based decoding, where at each time instant there are nodes describing the state of the encoder and from each node there are branches. Branches depend on the current input to the encoder. For convolution codes construction of the trellis is fairly simple. The bits stored in the shift registers or the memory elements of the convolution encoder determine the state of the encoder. For a linear block code $[n, k]$ the trellis can be constructed using the parity check matrix of the corresponding linear block code [2]. The state at time t for a linear block encoder is given by

$$S_t = S_{t-1} + c_t h_t, \quad (1)$$

where $t = 1, 2, \dots, n$. c_t is the t^{th} bit of the codeword and h_t is the t^{th} column vector of parity check matrix \mathbf{H} . Each state S_t is a vector of length $(n - k)$. The total number of all possible states are 2^{n-k} . Assume the encoder is initialized to an all-zero state or null state. Thus Eq. 1 becomes

$$S_t = \sum_{i=1}^t c_i h_i. \quad (2)$$

Consider the parity check matrix \mathbf{H} of a $[6, 3, 3]$ code, which we use primarily in this paper to demonstrate the algorithm:

$$\mathbf{H} = \begin{bmatrix} 0 & 1 & 1 & 1 & 0 & 0 \\ 1 & 0 & 1 & 0 & 1 & 0 \\ 1 & 1 & 0 & 0 & 0 & 1 \end{bmatrix}.$$

Based on the \mathbf{H} , we show the trellis of the $[6, 3, 3]$ code in Fig. 1. From each node, there are two possible branches for each c_i , where $c_i \in \{0, 1\}$. The trellis is irregular as the linear block encoder is a time-varying Markov source. Although a state diagram is not possible for the linear block code encoder, trellis can be constructed as shown. Thus, Viterbi decoder can also be used to decode linear block codes. Each possible path through the trellis is a valid codeword. A valid codeword of a linear block code must be a member of the codespace \mathcal{C} . This codespace has a property that each member c of \mathcal{C} must satisfy $c\mathbf{H}^T = 0_{1 \times n}$. The codespace is thus

$$\mathcal{C} = \{c : c\mathbf{H}^T = 0_{1 \times n}\}. \quad (3)$$

Also along with the null state initialization, the final state of the encoder should also be a null state only. This constraint of the trellis determines the valid paths. We discard the branches which do not end up in the final null state, as they do not produce a valid codeword. The Viterbi decoder evaluates the Hamming distance between the t^{th} bit of the received erroneous vector and the valid branches at each of the t time instances. The Hamming distance evaluated for each branch is assigned as its partial path metric. The total path metric of a valid path is the total sum of all the partial path metrics of the path. The path with the least total path metric is the decoded codeword. This path thus refers to the codeword having the least Hamming distance with respect to the received erroneous vector. We use the QAOA introduced by Farhi *et al.* [11] to find the paths with least path metric in the trellis. We now briefly mention the QAOA and the variational principle used in the algorithm we propose.

3 The Variational Principle and Quantum Approximate Optimization

For physical systems sometimes the exact solution of the system Hamiltonian is not known analytically. The variational principle is an approximation method for determining the ground state energy of the system. The ground state is approximated by a parameterized educated guess called ansatz. The expectation value of the system Hamiltonian is the cost, which is minimized by varying the parameter of the ansatz. Upper bound for the ground state energy E_g of the quantum system with Hamiltonian H is

$$E_g \leq \langle \psi(\theta) | H | \psi(\theta) \rangle, \quad (4)$$

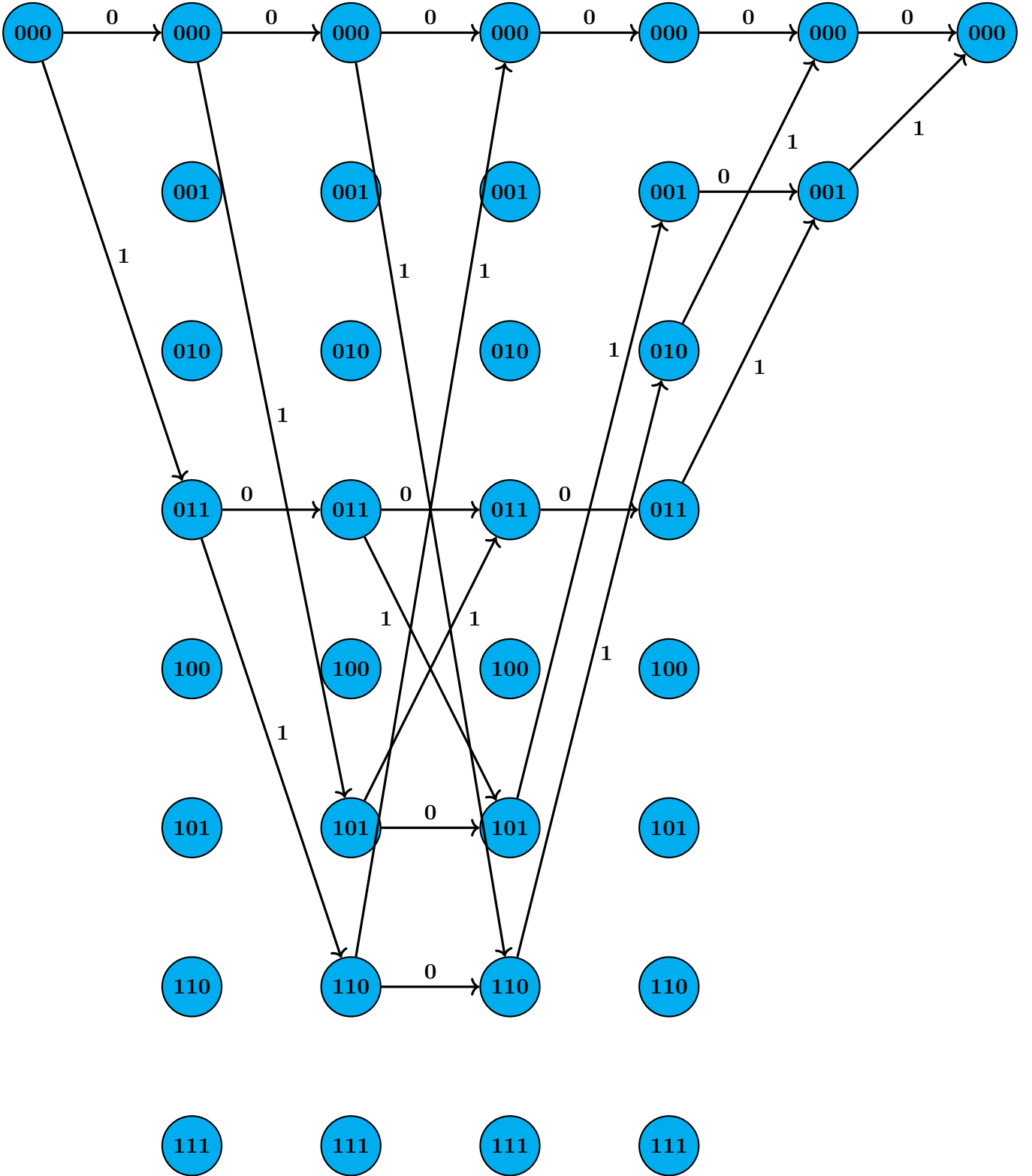


Figure 1: Trellis of $[6,3,3]$ Linear Block Code Encoder. The encoder initializes and terminates in the null state. There are total 8 possible paths shown in the trellis, which satisfy the initialization and termination condition. From each state the encoder can jump into any of the two possible states depending upon the input c_i at i^{th} time instant.

where $\psi(\theta)$ is the ansatz. The parameter θ is optimized to keep the expectation value in Eq. 4 as close to the actual ground state energy. This idea is extended in the hybrid classical-quantum algorithm, where the expectation value of the cost Hamiltonian is extracted from repeated calls on a quantum computer and the optimization is done using a classical optimizer. The QAOA is a variational quantum algorithm, where instead of tweaking the ansatz we optimize the parameters of the PQC, which essentially represents a circuit of time evolution unitary gates of the Hamiltonian, related to the optimization problem.

3.1 Quantum Approximation Optimization Algorithm

Quantum Approximation Optimization algorithm or QAOA can approximately solve combinatorial optimization problems like MAX-CUT problem [11], and Travelling Salesman Problem [21]. Objective of the QAOA is to encode an optimization problem into a problem of finding the ground state of a problem related Hamiltonian. The ground state of a Hamiltonian refers to the state with minimum eigenvalue. QAOA utilizes both quantum and classical methods to obtain the ground state of an observable Hamiltonian. The optimization problem is generally expressed in terms of a Boolean or pseudo-Boolean function. The QAOA uses PQC to evaluate this cost function by evaluating the expectation value of the corresponding Hamiltonian. Then a classical optimizer is used to tweak the parameters, such that we achieve the minimized expectation value of the Hamiltonian. A general schematic representation of QAOA is shown in Fig. 2. The encoding of the cost functions of any problem into a diagonal Hamiltonian is the first key step of QAOA. The cost function, in general is a map $f : \{0, 1\}^n \rightarrow \mathbb{R}$ defined by

$$f(x) = \sum_{i=1}^{\alpha} w_i C_i(x), \quad (5)$$

where x is a n bit string and $w_i \in \mathbb{R}$, and $C_i(x)$ is a Boolean function that takes the n bit string as input and gives a binary output. We note that $C_i(x)$ acts locally on some of the bits of the n bit string x . The representation in Eq. 5 suggests that the total cost function consists of a weighted sum of several local Boolean functions, where α is the total number of such local terms. The locality of each Boolean function is the locality of its acting domain. This weighted sum representation of the cost function $f(x)$ is a pseudo-Boolean function. For the problem of Viterbi decoding the cost function is also a pseudo-Boolean or real function. It evaluates the Hamming weight between two vectors.

The diagonal Hamiltonian corresponding to the cost function $f(x)$ should be constructed such that

$$H_f |x\rangle = f(x) |x\rangle, \quad (6)$$

where $|x\rangle$ is eigenstate of H_f with the eigenvalue $f(x)$. This H_f is called the cost Hamiltonian. This suggests that the eigenvalues of the cost Hamiltonian is the real value of the cost function defined in Eq. 5.

The expectation value of this Hamiltonian refers to the cost that must be minimized. In PQC time evolution of the cost Hamiltonian is defined as

$$U_f(\gamma) = e^{-i\gamma H_f}, \quad (7)$$

where we call it the cost unitary, with γ as the evolution parameter of H_f . A single layer of PQC contains another unitary along with the $U_f(\gamma)$. It is called the mixer

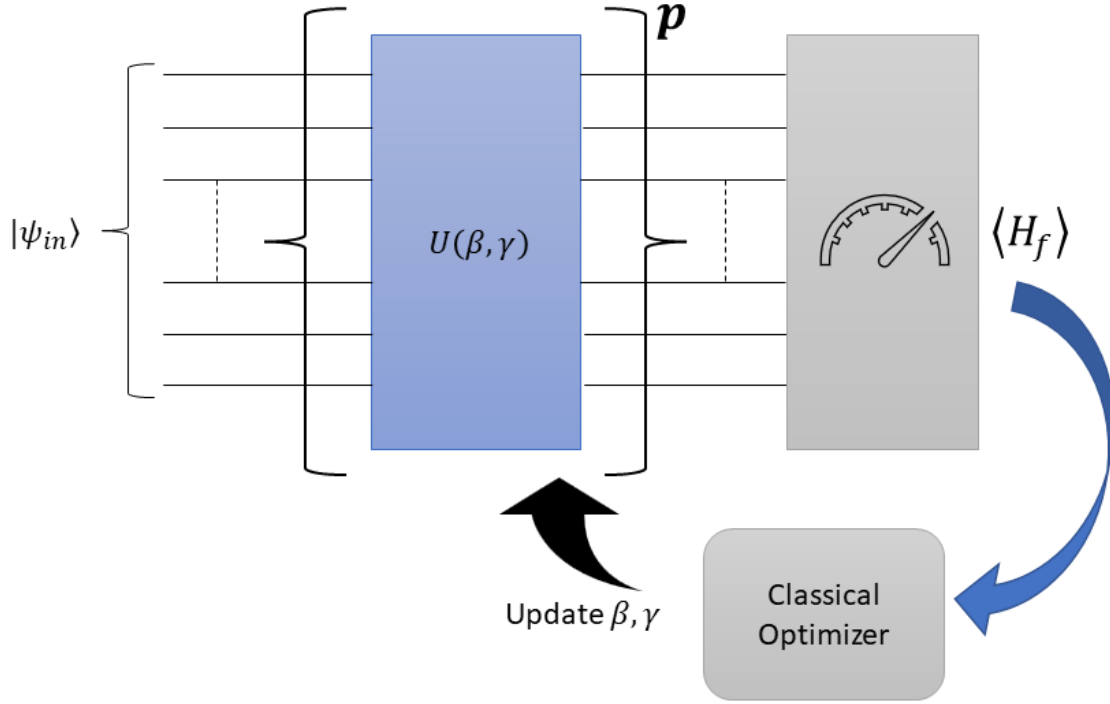


Figure 2: This is a schematic representation of QAOA. $U(\beta, \gamma)$ is the parameterized unitary, $U(\beta, \gamma) = U_f(\gamma)U_m(\beta)$. The PQC consists of p repetitions of the parameterized unitary, and β, γ are two sets of parameters. The expectation value of the cost Hamiltonian H_f is minimized by a classical optimizer and gives a feedback for the updated parameters to the PQC.

and is defined as

$$U_m(\beta) = e^{-i\beta H_m}, \quad (8)$$

where H_m is the mixer Hamiltonian and β is the evolution parameter of H_m . The mixer Hamiltonian is used to ensure a non uniform evolution of the initial state over which $U_m(\beta)$ and $U_f(\gamma)$ is applied repeatedly. The initial state is an educated guess of the ground state of H_f . It is called the ansatz. The ansatz we generally use in QAOA is any valid eigenstate of H_f or an equal superposition of all of them. For example if all the computational basis states of a n qubit system are the eigenstates of the H_f , then the most useful ansatz will be the equal superposition of all the basis states. This can be achieved in unit depth operation of Hadamard gates on n qubits and the ansatz is expressed as

$$|\psi_{in}\rangle = \frac{1}{\sqrt{2^n}} \sum_{i=1}^{2^n} |i\rangle. \quad (9)$$

On this ansatz, we operate parameterized unitaries U_m and U_f repeatedly to amplify the probability of the solution state. The solution state is the state corresponding to the decoded codeword, which gives the minimum value for the cost function. If the unitaries are being applied for p times, the output state is defined as $|\psi(\beta, \gamma)\rangle$, where β, γ are the set of parameters used in the PQC. Expanding the parameter set the output state is given as,

$$|\psi(\beta_1, \beta_2, \dots, \beta_p, \gamma_1, \gamma_2, \dots, \gamma_p)\rangle = e^{-i\gamma_p H_f} e^{-i\beta_p H_m} e^{-i\gamma_{p-1} H_f} e^{-i\beta_{p-1} H_m} \dots \\ \dots e^{-i\gamma_2 H_f} e^{-i\beta_2 H_m} e^{-i\gamma_1 H_f} e^{-i\beta_1 H_m} |\psi_{in}\rangle, \quad (10)$$

The parameters $\beta = (\beta_1, \beta_2, \dots, \beta_p)$ and $\gamma = (\gamma_1, \gamma_2, \dots, \gamma_p)$ requires optimization classically. A properly optimized PQC will output the decoded solution state with higher probability.

Eq. 6 implies $\langle f \rangle = \langle H_f \rangle$, where $\langle f \rangle$ is the average of the cost function and $\langle H_f \rangle$ is the expectation value of the observable H_f evaluated over the quantum state $|\psi(\beta, \gamma)\rangle$. Running the operation of Eq. 10 in a quantum computer multiple times and measuring the output gives an expectation value

$$\langle \psi(\beta, \gamma) | H_f | \psi(\beta, \gamma) \rangle = \sum_{i=1}^{2^n} p_i f(x_i), \quad (11)$$

where p_i denotes the probability of the i^{th} basis state. Minimizing this expectation value using a classical optimizer, gives us the optimized parameters. The optimized parameters when used again according to Eq. 10 on a quantum computer, it leads to an increment in the probability of the solution state compared to the non-solution states. But finding good parameters are exhausting. Further the choosing initial set of parameters γ and β used in the PQC are also essential, which we discuss next.

3.2 Works related to the hurdles of QAOA

Often QAOA fails to produces optimized solution to a problem [1]. Hardware-efficient ansatzes are used in PQC due to their simplicity and efficiency. But random initialization of parameters of this hardware efficient PQC is the reason for the emergence of barren plateaus [19]. A barren plateau refers to a flat optimization landscape, which is quantified by exponentially vanishing variance of the gradients of the cost function. In their work McClean *et al.* showed that these barren plateaus occur for deep versions of the randomly initialized PQC, essentially the depth D is at least $D = \mathcal{O}(\text{poly}(n))$ for the occurrence of these plateaus [19]. Deep versions of PQC refers to circuits having higher p . A flatter optimization landscape for deep circuits suggests that the success in finding a good solution strictly depends on the initial guess of the parameters. But as such, there are no optimal techniques for it. Cerezo *et al.* showed that the occurrence of barren plateaus is also cost function dependent [8]. The authors showed that if the cost function Hamiltonian is global, then barren plateaus will occur even for shallow-depth circuits and there is no escape from it. But the gradients vanish at worst polynomially for lower depths up to a depth of $D = \mathcal{O}(\log(n))$, if the defined cost function Hamiltonian is local. They also proved that the gradients vanish exponentially if the depth is $D = \mathcal{O}(\text{poly}(n))$ and beyond. This renders the PQC trainable for shallow circuits. We use this fact to construct a trainable parameterized quantum circuit for our hybrid Viterbi decoder.

The inevitability of barren plateaus in higher-depth regions is worrying because this is the region where we get the solutions of the algorithm with high probability. We have formulated a uniform parameter optimization technique, which gives us efficient results for finding good solutions even for lower-depth PQC. This is an approach to avoid barren plateaus and also makes the PQC efficient for NISQ devices. Also, we formulate the cost function such that its Hamiltonian mapping is local. This makes our PQC more trainable and gives us an efficient quantum algorithm for Viterbi decoding. We now formally develop the hybrid Viterbi decoder.

4 Quantum Classical Hybrid Viterbi Decoder

We map the Viterbi decoding problem into its variational quantum counterpart. To design the quantum circuit which essentially evaluates the cost function, we need to construct the cost and mixer Hamiltonians. These two must be non-commuting with each other. If H_f and H_m does not commute, they does not posses simultaneous eigenstates. This ensures a change in amplitudes of the initial state on time evolution.

4.1 Construction of the Cost Hamiltonian

Based on the discussion in Section 3.1, we propose the cost function for the Viterbi decoder as

$$f(x) = \sum_{i=1}^n x_i \oplus r_i, \quad (12)$$

where r_i is the i^{th} bit of the received vector, x_i is the i^{th} bit of the codeword, \oplus is the modulo 2 addition, and n is the total number of bits in the codeword. The function in Eq. 12 is a pseudo-Boolean function. It is a real function, which is a weighted sum of Boolean functions of the form given in Eq. 5. We also note that the cost function we proposed is local. The cost function defined in Eq. 12 takes the n bit codeword as input and returns the Hamming weight between the codeword and the received vector, as the output. The unique diagonal Hamiltonian representation of the pseudo-Boolean function is represented by a weighted sum of Pauli-Z operators. The terms in the summation correspond to the Fourier expansion of the function [15]. The Hamiltonian corresponding to Eq. 12 is

$$H_f = \sum_{i=1}^n \left(\frac{1}{2} \mathbf{I} - \frac{1}{2} Z_i^x Z_i^r \right), \quad (13)$$

where x represents the contents of a qubit register corresponding to the bits of the codeword. The cost Hamiltonian of Eq. 13 is a local observable. Each bit of the codeword $(x_1, x_1, x_3, \dots, x_n)$ is mapped into the corresponding qubit in the x register. r is the ancilla register representing the bits of the received erroneous vector. Each bit of the received vector $(r_1, r_1, r_3, \dots, r_n)$ is mapped into the corresponding qubit of the r register. Z_i^x is the Pauli-Z operator acting on the i^{th} qubit of the register x . Similarly, Z_i^r is the Pauli-Z operator acting on the i^{th} qubit of the register r . Now we derive the expression of the Hamiltonian in Eq. 13 in a simple way.

Consider a Boolean function $C(x) : \{-1, 1\}^n \rightarrow \{-1, 1\}$. The Fourier expansion of the function is [15]

$$C(x) = \sum_{S \subseteq [n]} \hat{C}(s) \prod_{i \in S} x_i, \quad (14)$$

$$= \sum_{S \subseteq [n]} \hat{C}(s) \chi_S, \quad (15)$$

where $\chi_S = \prod_{i \in S} x_i$, is the parity function and can be mapped to Pauli-Z operators of the form $\prod_{i \in S} Z_i$; $[n]$ is defined as the set of n elements, such that, $[n] = \{-1, 1\}^n$. This mapping is obvious when we work in the computational basis states, since $|0\rangle$ and $|1\rangle$ are the eigenstates of Pauli-Z with eigenvalues $+1$ and -1 respectively. Thus, the Hamiltonian

corresponding to the Boolean function $C(x)$ is

$$H_C = \sum_{S \subseteq [n]} \hat{C}(s) \prod_{i \in S} Z_i, \quad (16)$$

where $\hat{C}(s)$ are the Fourier coefficients and solely depend on the value of the function. Eq. 14 is a real multilinear polynomial, which is further simplified as,

$$\begin{aligned} C(x) &= \sum_{a \in \{-1,1\}^n} C(a) \mathbb{I}(x), \\ &= \sum_{a \in \{-1,1\}^n} C(a) \left(\frac{1+a_1x_1}{2} \right) \left(\frac{1+a_2x_2}{2} \right) \dots \left(\frac{1+a_nx_n}{2} \right), \end{aligned} \quad (17)$$

here the sum runs over all possible combinations of a . If $C(x) : (\{-1,1\}^2 \rightarrow \{-1,1\})$, we define one such function as

$$C(x) = x_1 \oplus x_2, \quad (18)$$

where $x = (x_1, x_2)$. Now Eq. 17 becomes,

$$\begin{aligned} C(x) &= C(-1, -1) \left(\frac{1-x_1}{2} \right) \left(\frac{1-x_2}{2} \right) + C(-1, 1) \left(\frac{1-x_1}{2} \right) \left(\frac{1+x_2}{2} \right) \\ &\quad + C(1, -1) \left(\frac{1+x_1}{2} \right) \left(\frac{1-x_2}{2} \right) + C(1, 1) \left(\frac{1+x_1}{2} \right) \left(\frac{1+x_2}{2} \right). \end{aligned} \quad (19)$$

Putting the value of $C(x)$ as defined in Eq. 18, the Fourier expansion of Eq. 19 becomes

$$\begin{aligned} C(x) &= -1 \left(\frac{1-x_1}{2} \right) \left(\frac{1-x_2}{2} \right) + 1 \left(\frac{1-x_1}{2} \right) \left(\frac{1+x_2}{2} \right) \\ &\quad + 1 \left(\frac{1+x_1}{2} \right) \left(\frac{1-x_2}{2} \right) - 1 \left(\frac{1+x_1}{2} \right) \left(\frac{1+x_2}{2} \right), \\ &= -x_1x_2. \end{aligned} \quad (20)$$

It can be easily verified from the above equation that the multilinear expansion satisfies the definition of $C(x)$, given in Eq. 18. If the Range of the Boolean function is changed from $\{-1,1\}$ to $\{0,1\}$, the Fourier expansion of the function $C(x)$ derived in Eq. 20 becomes [15]

$$\begin{aligned} C'(x) &= \frac{1+C(x)}{2}, \\ &= \frac{1}{2}(1-x_1x_2). \end{aligned} \quad (21)$$

Now using the Hamiltonian mapping obtained in Eq. 16, we find the Hamiltonian for $C'(x)$ becomes

$$H_C = \frac{1}{2}(\mathbb{I} - Z_1Z_2). \quad (22)$$

This is also the cost Hamiltonian corresponding to the function $C(x)$, given in Eq. 18, because $C'(x)$ is the Fourier expansion of $C(x)$. We mention that the cost function for the Viterbi decoder $f(x)$ in Eq. 12 is just the weighted sum of $C(x)$, where $x = (x_i, r_i)$ and all the weights are 1. Thus, replacing the variables in Eq. 21 by $x_1 \rightarrow x_i$ and $x_2 \rightarrow r_i$ and then summing over i from 1 to n , Eq. 22 becomes $H_c \rightarrow H_f = \sum_{i=1}^n \left(\frac{1}{2}\mathbb{I} - \frac{1}{2}Z_i^x Z_i^r \right)$. This is the cost Hamiltonian of the Viterbi decoder we proposed in Eq. 13. Now along with the cost Hamiltonian, QAOA requires a mixer Hamiltonian. We now propose the correlation between the minimum Hamming distance of the code and the mixer Hamiltonian.

4.2 Construction of the Mixer Hamiltonian

Along with the cost unitary, a mixer unitary is also applied on the initial state. The states in the initial uniform superposition are the eigenstates of the cost Hamiltonian. So, only the cost unitary can not disturb the amplitude profile of the initial state. It only adds a phase to each of the states in the superposition without altering the probability profile of the individual states. The mixer Hamiltonian in that sense mixes the amplitudes. The mixer Hamiltonian corresponding to the mixer unitary must conserve the search space, which is essential in the proposed Viterbi decoding algorithm. In many applications of QAOA including the Viterbi decoding, the search space does not contain all the basis members of a n qubit system. This is a restricted search space and in such situations we must choose the mixer Hamiltonian that does not map the states outside the search space(\mathcal{C}). Thus, the mixer unitary must conserve the same search space. Here our restricted search space is the codespace. But the mixer Hamiltonian must not have any eigenstates in the codespace either and this ensures the non commuting nature of the mixer Hamiltonian and the cost Hamiltonian.

The minimum Hamming distance of the codespace is defined as the minimum value of the Hamming distance between all pairs of the elements in that search space. We also assume there must be a null element in the search space and there are v elements in the search space with Hamming distance d with respect to the null element, where d is the minimum Hamming distance of the codespace. Now we state a theorem to generate a valid mixer for any restricted search space.

Theorem 1. *If \mathcal{C} is a restricted search space of a linear block code in a 2^n dimensional system and d is the minimum Hamming distance of \mathcal{C} , then the mixer Hamiltonian H_m is the sum of local Pauli-X operators, which maps the null element to any of the v elements with Hamming weight d :*

$$H_m = \sum_{c:w_H(c)=d} \prod_{j:c_j=1} X_j. \quad (23)$$

Proof. To prove Theorem 1, we first define the framework of the mixer Hamiltonian. Let $|\psi\rangle$ be the initial guess solution state of the variational algorithm. We choose it to be the equal superposition of all the states from the codespace. This makes the initial guess feasible. The initial guess is

$$\begin{aligned} |\psi_{in}\rangle &= U_g |0\rangle^{\otimes n}, \\ &= \frac{1}{\sqrt{2^k}} \sum_{i \in \mathcal{C}} |i\rangle. \end{aligned} \quad (24)$$

We can also choose any $i \in \mathcal{C}$. That will also be a valid initial guess. The mixer is defined as $e^{-i\beta H_m}$ in Eq. 8. The mixer must satisfy the constraint of mapping elements into the codespace only and as H_m is Hermitian, the mapping of both the mixer and the mixer Hamiltonian is same.

$$\begin{aligned} U_m |\psi_{in}\rangle &\in \mathcal{C}, \\ \implies e^{-i\beta H_m} |\psi_{in}\rangle &\in \mathcal{C}, \\ \implies H_m |\psi_{in}\rangle &\in \mathcal{C}. \end{aligned} \quad (25)$$

Detailed proof of this equivalence is given in Appendix A.1. The above Eq. 25 implies the feasible mapping within the codespace by the mixer Hamiltonian. To follow this constraint

we propose the Hamiltonian be

$$H_m = \sum_{x_j, x_k \in \mathcal{C}} g_{j,k} |x_k\rangle \langle x_j|, \quad (26)$$

$$\text{where, } g_{j,k} = \begin{cases} 1 & \forall (j,k) : d(x_j, x_k) = d. \\ 0 & \text{otherwise.} \end{cases} \quad (27)$$

Eq. 26 and Eq. 27 suggests that H_m must contain the tensor product of local Pauli operators, such that individually they map any state to a state with Hamming distance d . g is the matrix which determines this valid transitions through Eq. 27, and has a dimension $\dim(\mathcal{C}) \times \dim(\mathcal{C})$. Thus for any given (n, k, d) code g can be constructed. Using the matrix g and expanding the matrices for each term of Eq. 26, it is verified that

$$H_m = \sum_{j,k \in \mathcal{C}} g_{j,k} |x_k\rangle \langle x_j| = \sum_{c: w_H(c)=d} \prod_{j: c_j=1} X_j. \quad (28)$$

Now for any linear block code using $|x_j\rangle = |x_0\rangle = |0\rangle^{\otimes n}$, Eq. 26 implies:

$$\begin{aligned} H_m |0\rangle^{\otimes n} &= \sum_{x_k \in \mathcal{C}} g_{0,k} |x_k\rangle \langle 0|^{\otimes n} |0\rangle^{\otimes n}, \\ &= \sum_{x_k: d(x_0, x_k)=d} |x_k\rangle. \end{aligned} \quad (29)$$

□

The mapping is thus verified. Each term of Eq. 23 or Eq. 26 is mapping the elements in \mathcal{C} into another element in the same \mathcal{C} , with Hamming distance d . From the Eq. 26 it is fairly clear that the depth of the PQC will increase according to the minimum Hamming weight and structure of the code. If in the codespace there are more elements with minimum Hamming weight respective to the null element, the depth will increase. Thus PQC for different linear block codes may have higher depths. We now focus on incorporating these two Hamiltonian into its corresponding unitary gates and construct the parameterized quantum circuits for decoding linear block codes using the Viterbi decoding method.

4.3 Parameterized Quantum Circuit design for [6,3,3] Linear Block Code

We now design the PQC for the [6, 3, 3] code. The initial state is an equal superposition of all the codewords for the [6, 3, 3] code. Thus, the restricted search space is of dimension 2^3 . We can generate this superposition using a unitary operator constructed from the generator matrix of the [6, 3, 3] code. The generator matrix of this [6, 3, 3] code is

$$\mathbf{G} = \begin{bmatrix} 1 & 0 & 0 & 0 & 1 & 1 \\ 0 & 1 & 0 & 1 & 0 & 1 \\ 0 & 0 & 1 & 1 & 1 & 0 \end{bmatrix}. \quad (30)$$

The unitary operator U_g , which generates an equal superposition of all codewords of the [6, 3, 3] code belonging to codespace \mathcal{C} is [16]

$$U_g = \prod_{4 \leq i \leq 6} \left(\prod_{1 \leq j \leq 3, G_{ji}=1} CX_{j,i} \right) \prod_{1 \leq j \leq 3} H_j, \quad (31)$$

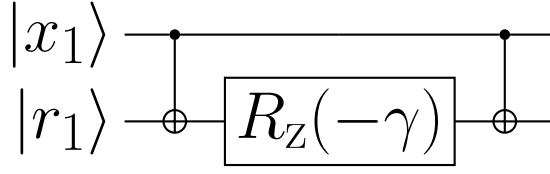


Figure 3: Circuit for $e^{i\frac{\gamma}{2}Z_1^x Z_1^r}$. This is one of the terms from Eq. 33. $|x\rangle$ refers to the codeword register and $|r\rangle$ refers to the ancilla register. $R_z(-\gamma)$ is the single qubit rotation gate about the z axis, $R_z(-\gamma) = e^{i\frac{\gamma}{2}Z}$.

where $CX_{j,i}$ is the controlled Pauli-X gate. Using this U_g on a set of all qubits initialized to $|0\rangle$ generates the desired uniform superposition of the elements in codespace \mathcal{C} . The initial state can be written as

$$\begin{aligned} |\psi_{in}\rangle &= U_g |0\rangle^{\otimes 6}, \\ &= \frac{1}{\sqrt{2^3}} \sum_{i \in \mathcal{C}} |i\rangle. \end{aligned} \quad (32)$$

We require additional six more ancilla qubits which store the information of the received erroneous vector. All the ancilla qubits are initialized to the $|0\rangle$ state. Whenever a bit of the received vector is 1, we apply a Pauli-X gate on the corresponding qubit. The reason we incorporate these ancillas lies in the structure of the cost function Hamiltonian H_f in Eq. 13. The unitary corresponding to the H_f is

$$\begin{aligned} U_f(\gamma) &= e^{-i\gamma H_f}, \\ &= e^{-i\gamma \sum_{i=1}^n (\frac{1}{2}I - \frac{1}{2}Z_i^x Z_i^r)}, \\ &= \prod_{i=1}^n e^{i\frac{\gamma}{2}Z_i^x Z_i^r}, \end{aligned} \quad (33)$$

where $n = 6$ is the number of bits in the codeword and γ is a scalar evolution parameter of H_f . The identity operator contributes a global phase to the state. As the global phase has no physical effect on the quantum state, the effect of the identity operator is redundant in the PQC. Eq. 33 essentially represents a connection between the respective qubits of register x and r . For example, we demonstrate the quantum circuit of one such term $e^{i\frac{\gamma}{2}Z_1^x Z_1^r}$ from Eq. 33 in Fig. 3. This connects x_1 to r_1 .

The other unitary we need to apply before the cost unitary is the mixer H_m . For which we first describe the mixer Hamiltonian for the $[6, 3, 3]$ linear block code. The $[6, 3, 3]$ code generated by the generator matrix of Eq. 30 is

$$\mathcal{C} = \{|000000\rangle, |001110\rangle, |010101\rangle, |100011\rangle, |011011\rangle, |110110\rangle, |101101\rangle, |111000\rangle\}.$$

Using Eq. 23 from Theorem 1 we find that the mixer Hamiltonian for the $[6, 3, 3]$ code is

$$H_m = X_1 X_2 X_3 + X_1 X_5 X_6 + X_3 X_4 X_5 + X_2 X_4 X_6. \quad (34)$$

Thus, the mixer unitary (mixer) defined as $U_m(\beta) = e^{-i\beta H_m}$ is of the form

$$\begin{aligned} U_m(\beta) &= e^{-i\beta(X_1 X_2 X_3 + X_1 X_5 X_6 + X_3 X_4 X_5 + X_2 X_4 X_6)}, \\ &= e^{-i\beta X_1 X_2 X_3} e^{-i\beta X_1 X_5 X_6} e^{-i\beta X_3 X_4 X_5} e^{-i\beta X_2 X_4 X_6}, \end{aligned} \quad (35)$$

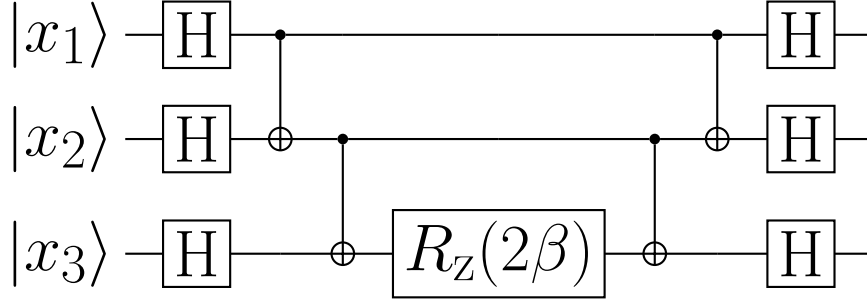


Figure 4: This is the circuit for $e^{-i\beta X_1 X_2 X_3}$. We exploit the fact that $H \otimes H \otimes H e^{i\beta Z_1 Z_2 Z_3} H \otimes H \otimes H = e^{i\beta X_1 X_2 X_3}$.

where β is a scalar evolution parameter of H_m . We demonstrate the quantum circuit for the term $e^{-i\beta X_1 X_2 X_3}$ from Eq. 35 in Fig. 4. Following this pattern of CNOT, Hadamard and R_Z gate we construct circuits for the other exponents of the product of Pauli-X gates. Finally, U_f of Eq. 33 and U_m of Eq. 35 form the unit layer of the PQC of QAOA for the Viterbi decoder of the $[6, 3, 3]$ code. We are referring to a single operation of the cost unitary U_f , Eq. 33 and a single operation of the mixer, Eq. 35 as a single unitary layer of QAOA. This unit layer circuit is shown in Fig. 5. This one layer of unitary is repeated on the initial quantum state $|\psi_{in}\rangle$ of Eq. 32. If repeated p times, the final state becomes $|\psi(\beta_1, \beta_2, \dots, \beta_p, \gamma_1, \gamma_2, \dots, \gamma_p)\rangle$, as given in Eq. 10. The PQC requires a classical optimizer to optimize these parameters for finding the minimum of the cost function. But as discussed in Section 3.2, finding good parameters for the PQC is difficult. To overcome this difficulty, we propose an uniform parameter optimization method, which has better efficiency for finding good parameters in shallow depth.

5 Proposed Uniform Parameter Optimization (UPO) Strategy

Due to the hurdles we discussed in Section 3.2, it is important to develop strategies for finding good parameters of the PQC. This will ensure proper minimization of the cost function given in Eq. 11. There are two such strategies discussed by Lee *et al.* [17]. One of them is the random initialization method, which assumes multiple random initialization of the parameters to evaluate an average of the minimum approximation ratio, which is defined as

$$\alpha = \frac{f(\psi(\beta, \gamma))}{f_{\min}}, \quad (36)$$

where $\psi(\beta, \gamma)$ is the string representation of the state prepared by the PQC, Eq. 10. This process is repeated and the best set of parameters with least value of average α is chosen as the best fit for the parameters. Another strategy the authors discussed is parameters fixing strategy, which we denote as FPO. In FPO at each p , the parameters are optimized for q random initialization. Parameters giving minimum α are chosen as the optimized parameters for that particular p and then p is increased. We show that this approach of FPO offers very little assurance in finding solutions.

We suggest training the PQC with each parameter of different layers being equal for the mixer and the cost unitaries respectively. It implies

$$\beta_1 = \beta_2 = \dots = \beta_p = \beta_o \text{ and } \gamma_1 = \gamma_2 = \dots = \gamma_p = \gamma_o. \quad (37)$$

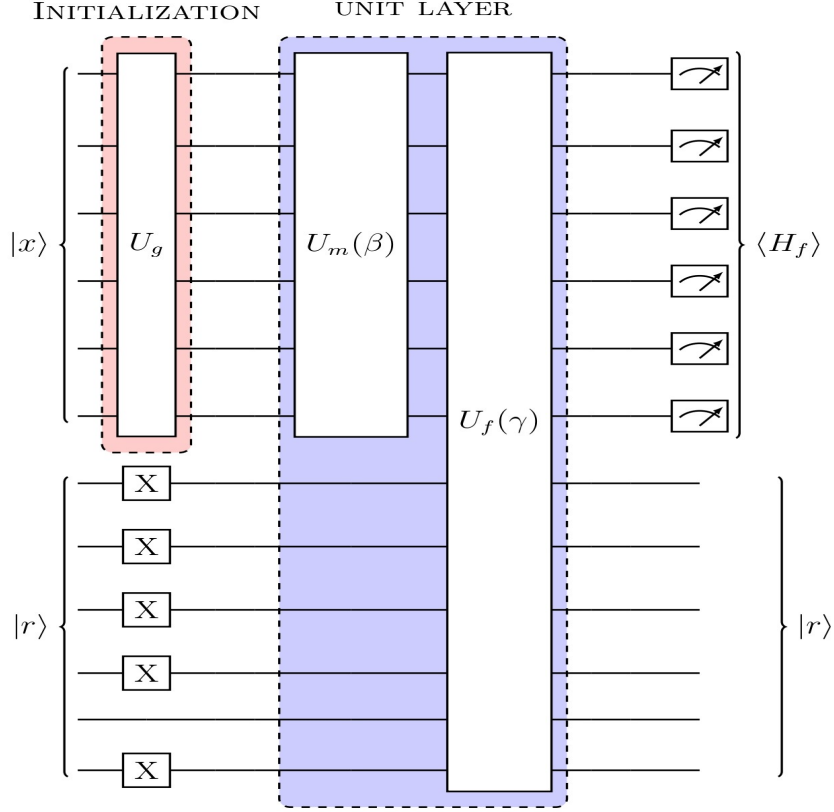


Figure 5: This is the circuit for an unit layer ($p = 1$) of QAOA applied on the initial state of the PQC. $|x\rangle$ is the register representing codeword bits. $|r\rangle$ is the register representing the ancilla bits corresponding to the received vector. We show here the circuit with $r = |111101\rangle$. U_g creates the valid initial state $|\psi_{in}\rangle$ of Eq. 32. An unit layer of QAOA consists of a single application of the mixer $U_m(\beta)$ Eq. 35 and the cost unitary $U_f(\gamma)$ Eq. 33. The mixer unitary is applied on the codeword register only, following the Theorem 1. The detailed circuit for the mixer and cost unitary is shown in Appendix A.2 and Appendix A.3 respectively. Expectation value of the cost Hamiltonian is obtained by Measuring the codeword register through repeated calling of the PQC.

We call this uniform parameter optimization (UPO). We train the parameterized quantum circuit for a fixed p with all the p mixer parameters having the value β_o and all the p cost unitary parameters having the value γ_o . There are q random initialization and each q set of $\{\beta_o, \gamma_o\}$ is applied to evaluate the cost $\langle H_f \rangle$ over the $|\psi(\beta, \gamma)\rangle$, where the set of parameters β and γ satisfies Eq. 37. Then we choose the best set of parameters as the optimized parameters, which has the minimum approximation ratio (α), which is defined in Eq. 36. We observe that the above method, namely UPO, can potentially obtain better parameters for the PQC than the parameter fixing strategy or FPO. We present the detailed uniform parameter optimization method for a generalized $[n, k, d]$ linear block code in Algorithm 1.

5.1 Performance Analysis of the UPO

We compare our uniform parameter optimization (UPO) with the fixed parameter optimization (FPO) technique suggested by Lee *et al.* [17] for obtaining good parameters. We apply it to find the least path from the trellis of a $[6, 3, 3]$ code upon receiving the erroneous vector $r = 111011$. Further, we analyse the performance of the two strategies by tracing

Algorithm 1 Proposed Uniform Parameter Optimization for the Hybrid Viterbi Decoder

1: Initialize the state is uniform superposition of all the elements of the codespace \mathcal{C} .

$$\begin{aligned} |\psi_{in}\rangle &= U_g |0\rangle^{\otimes n} \\ &= \frac{1}{\sqrt{2^k}} \sum_{i \in \mathcal{C}} |i\rangle \end{aligned} \quad (38)$$

2: Add ancilla qubits and apply Pauli- X gates in appropriate positions to represent the received erroneous vector.

$$\begin{aligned} |\psi_{in}\rangle &\rightarrow |\psi_{in}\rangle \otimes \prod_{j: wt(r_j)=1} X_j^r |0\rangle^{\otimes n} \\ |\psi_{in}\rangle &\rightarrow |\psi_{in}\rangle \otimes |r\rangle \end{aligned}$$

3: Declare f, t_β, t_γ as array of variables.

4: **while** $k \leq q$ **do**

5: $\beta_o \rightarrow \text{random}, \gamma_o \rightarrow \text{random}.$

6: $|\psi_{in}\rangle \otimes |r\rangle \rightarrow |\psi(\beta, \gamma)\rangle \otimes |r\rangle = (U_f^p(\gamma_o) U_m^p(\beta_o) |\psi_{in}\rangle) \otimes |r\rangle$

7: Measure the n codespace (x) qubits.

8: Run the circuit for 2000 shots.

9: Use Eq. 11 and Eq. 12 to find the expectation value $\langle f \rangle = \langle H_f \rangle = \sum_{i \in \mathcal{C}} \frac{m_i}{\text{shots}} f(i).$

10: Optimize $\langle f \rangle$ and store the optimized parameter in t_β and t_γ respectively and the optimized expectation value in f .

11: **end while**

12: **for** k in $f[k]$ **do**

13: **if** $f[k] : \min \left(\frac{f[k]}{f_{\min}} \right)$ **then**

14: $p_1 = t_\beta[k]$ and $p_2 = t_\gamma[k].$

15: **end if**

16: **end for, return** $p_1, p_2.$

out the occurrence of the actual solution state which is $|011011\rangle$, out of 2000 simulation shots for 10 training simulations. We observe that in Fig. 6 at each simulation instance after training the PQC with the UPO method, the actual solution has strikingly high occurrences with approximately 1500 occurrences out of 2000 shots. This shows the effectiveness of the proposed strategy towards obtaining good parameters. Whereas the fixed parameter optimization is quite random in obtaining good parameters. We observe that there are instances where the fixed parameter optimization fails to obtain good parameters. 3rd, 5th, 6th and 9th instance of the training shown in Fig. 6b reflects the failures. Also, we note that our observation, as in Fig. 7 with sampling parameters from an increased sample space of $q = 20$ random initialization, does not give a better amplification of the solution state, than the uniform one.

The cost function of Eq. 12 is essentially the expectation value of the observable in

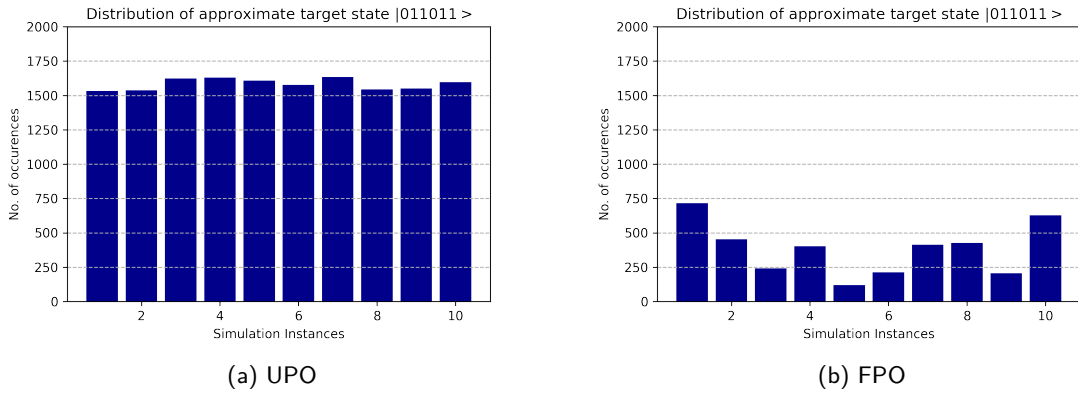


Figure 6: Here, in each case, the number of unitary layers is fixed to $p = 3$ for the decoder of a $[6, 3, 3]$ code. We choose to select the parameters with minimum approximation ratio as the good parameters out of $q = 5$ randomly initialized optimizations. We repeat each training method 10 times and run the PQC corresponding to each set of good parameters. We observe that upon tracing the nature of the probability profile of the actual solution state, the Uniform Parameter Optimization has better potential towards obtaining good parameters, as it amplifies the actual solution state and the pattern is outstandingly regular.

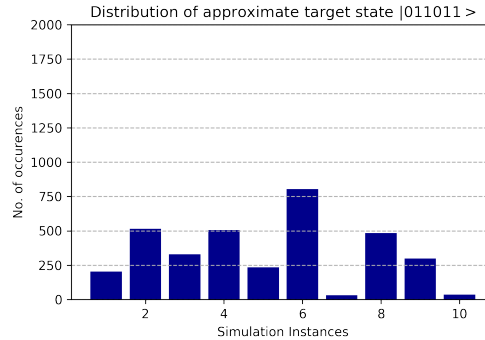
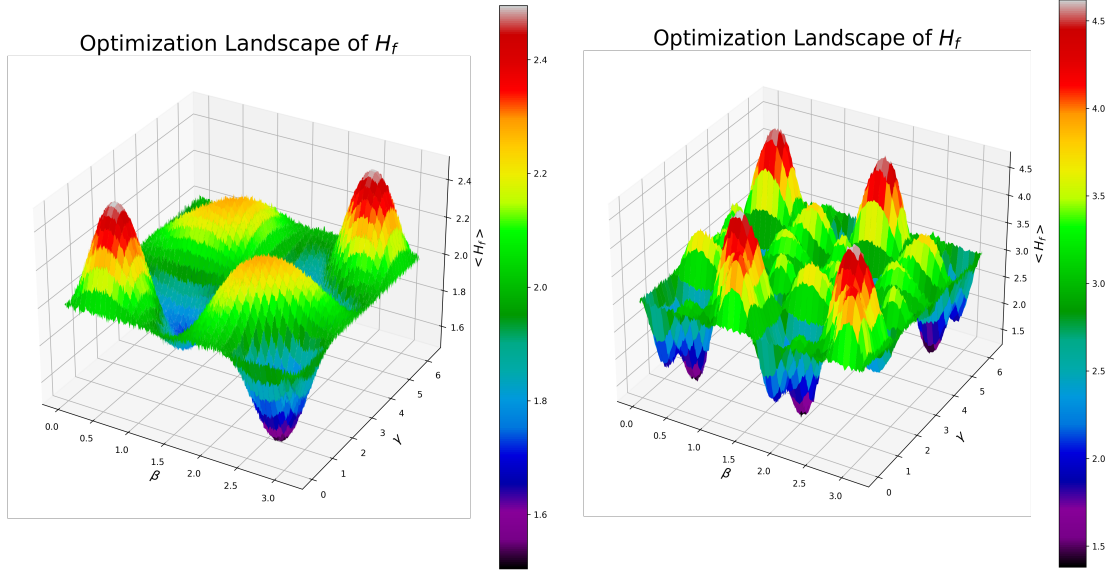


Figure 7: FPO for the $[6, 3, 3]$ code with $p = 3$. We chose to select the parameters which yield minimum approximation ratio as the good parameters out of $q = 20$ optimizations for each p . The occurrence of the state is quite random and thus is inconclusive.

Eq. 13. The state in which we calculate the expectation value is the state prepared by the



(a) Cost function landscape for the $[3, 2, 1]$ code with $p = 3$.

(b) Cost function landscape for the $[6, 3, 3]$ code with $p = 3$.

Figure 8: It is a landscape of the expectation value of the observable cost Hamiltonian H_f defined in Eq. 13, over the state prepared by the UPO trained PQC Eq. 39. The colour map signifies different surface heights for different colors. For both of the cases we observe no flat landscape.

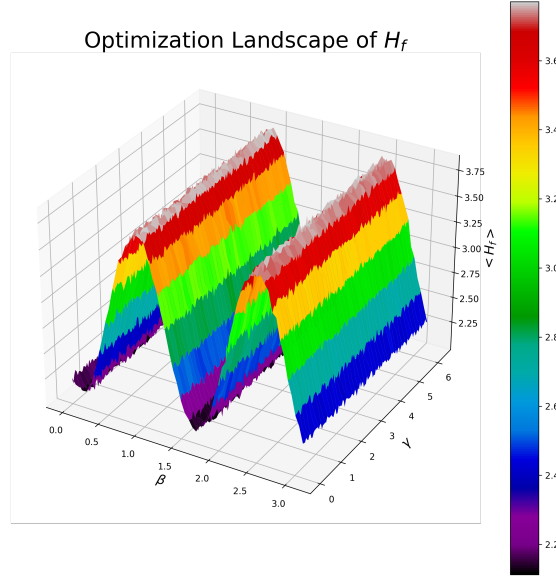


Figure 9: A typical approximation of the cost function landscape for the $[6, 3, 3]$ code with $p = 3$. The PQC is trained using FPO. We optimize β_1, β_2 and γ_1, γ_2 using FPO. Fixing them in those optimized values we observe the landscape due to the β_3 and γ_3 . Along gamma as we can see lies strips of zero gradients. These are shown by the strips of single colours along γ_3 . It signifies $\langle \frac{\partial f}{\partial \gamma_3} \rangle = 0$.

PQC. Thus the cost function which will be minimized is

$$f(\psi) = \langle \mathbf{0} | U_g^\dagger U_m^{\dagger p} U_f^{\dagger p} H_f U_f^p U_m^p U_g | \mathbf{0} \rangle,$$

where $|\mathbf{0}\rangle$ is the all-zero state and ψ refers to string representation of the state prepared

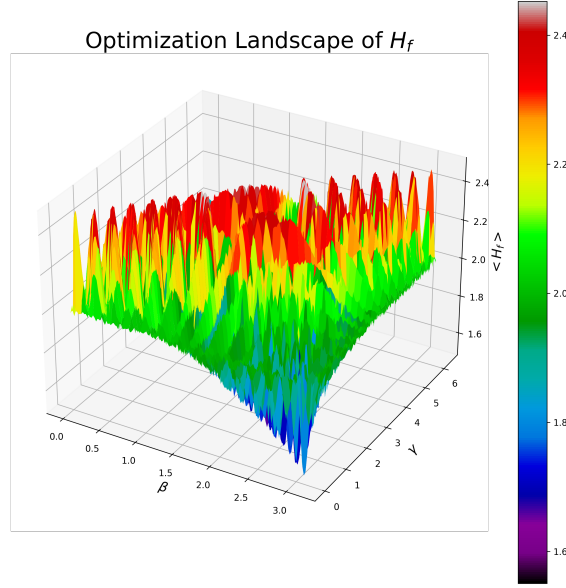


Figure 10: Cost function landscape for the $[3, 2, 1]$ code with $p = 15$. This is the landscape obtained using UPO. Here we also obtain a non uniform optimization landscape.

by the PQC

$$|\psi\rangle = |\psi(\beta, \gamma)\rangle = U_f^p(\gamma_o)U_m^p(\beta_o)U_g|\mathbf{0}\rangle. \quad (39)$$

In Fig. 8, we show the landscape of this cost function for $[3, 2, 1]$ and $[6, 3, 3]$ code, which is dependent on the uniformly parameterized quantum circuit. The optimization landscape is not flat and thus offers suitable optimization. This non-flat landscape explains the better efficiency of the UPO strategy. While it is expected that if one uses different parameters to prepare the PQC, different layers may cause the landscapes to shift towards the flat region. We visualize how barren plateaus still occur in our proposed Viterbi decoder if fixed parameter optimization is used. We chose again to work with the $[6, 3, 3]$ code. As the 6 variable function can not be visualized with ease, we try to fix the first 4 variables and plot the landscape for β_3 and γ_3 . This help us to analyse the occurrence of vanishing gradients due to β_3 and γ_3 . We observe in Fig. 9, for a fixed β_3 there are strips of zero gradients arising due to the parameter γ_3 . Thus, fixing parameters and optimizing offers no improvement in efficient optimization than random sampling.

We also test the optimization strategy for $p = 15$. In this case, also we observe that taking the same parameters for each unitary helps the classical optimizer find good parameters. We show the results in Fig. 11. In the case of higher-depth PQC also, we observe no flat landscapes that may cause trouble for the classical optimizers. We show the optimization landscape for higher depth PQC in Fig. 10. We now show the decoding results for other linear block codes and verify the multiple path tracing, all of which has least path metric.

5.2 Performance of the Hybrid Decoder

We discuss the uniform parameter optimization technique to determine a good parameter for the parameterized quantum circuit. After obtaining the parameters using UPO, we put them in the corresponding unitary layers and produce $|\psi(\beta, \gamma)\rangle$ of Eq. 10. The operation of the hybrid Viterbi decoder is summarized in the following 3 steps.

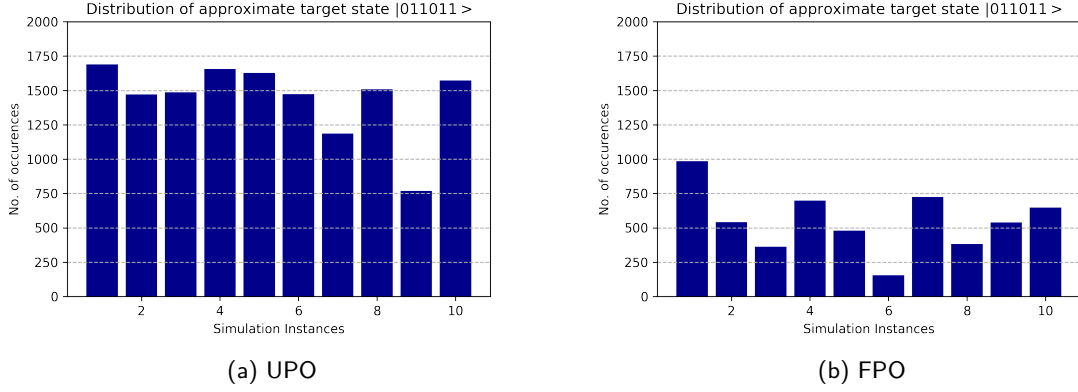


Figure 11: Comparison between Uniform and fixed optimization strategy for high depth PQC. The number of unitary repetitions is high in this PQC. We have shown 10 optimization instances and traced out how much probable the actual state with minimum path metric is. We chose $\mathcal{C} = [6, 3, 3]$, $p = 15$, $q = 5$.

1. Prepare an initial superposition of all the valid paths in the trellis using a generator unitary U_g , same as in Eq. 38.
2. Prepare a fixed depth p parameterized quantum circuit using repeating $U_m(\beta_o)$ and $U_f(\gamma_o)$ and train it using Uniform Parameter Optimization strategy.
3. Use the parameters obtained from the training in the PQC and measure the qubits.

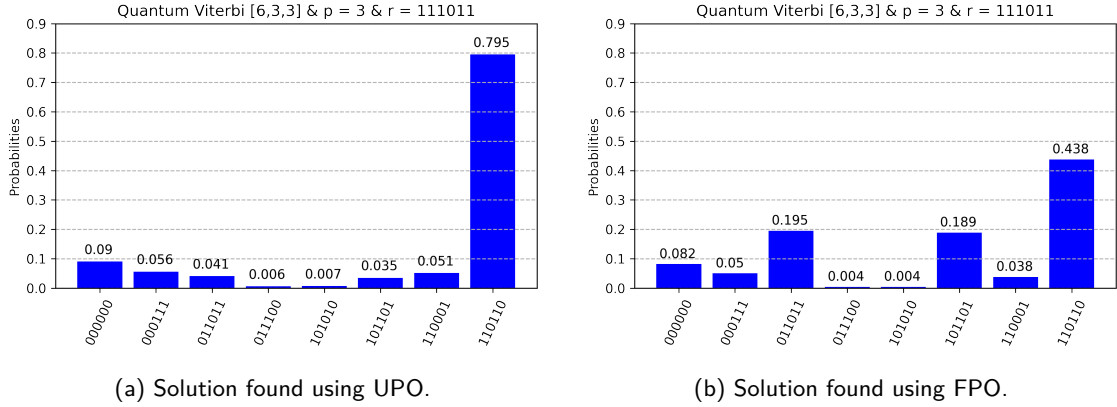


Figure 12: Results of the simulation obtained for Viterbi decoding by the QAOA using UPO. The code is $[6, 3, 3]$. We label the states with convention that the most significant bit is at the bottom. We apply $p = 3$ number of unitary layers. We sample out of $q = 5$ randomly initialized samples. Received vector is $r = 111011$. The amplified state refers to the decoded codeword or the path with the least metric in the trellis. For a fixed p and q , UPO offers better amplification than FPO.

In Fig. 12, we show the solution obtained with high probability for a $[6, 3, 3]$ code upon receiving an erroneous vector $r = 111011$. The state $|011011\rangle$ has the highest probability of occurrence and thus it is the solution we obtain using QAOA. The decoded path has a path metric $d(011011, r) = 1$. We note that this is indeed the path with minimum path metric corresponding to the received erroneous vector. We also show the amplification difference between the two optimization technique, which again points out the more acceptance of the UPO. We also apply the algorithm for a $[9, 4, 4]$ code upon receiving an erroneous

vector $r = 111011011$. The result is shown in Fig. 13. Here, we again use uniform parameter optimization to train the parameterized quantum circuit. The PQC we use has 3 unitary layers. The decoded codeword has unit path metric and is also the minimum among others. In another case where we took a $[3, 2, 1]$ code. Codespace of this code is $\mathcal{C} = \{000, 010, 101, 111\}$. For this code, if we receive the erroneous vector $r = 011$, the algorithm returns two states with high probability $|010\rangle$ and $|111\rangle$ as shown in Fig. 14. This suggests there are two paths with the least path metric, and this indeed matches the theory. It signifies that every path which has the minimum metric among all the paths will be opted out as the solution by the hybrid decoder. We now observe the results for the convolution codes.

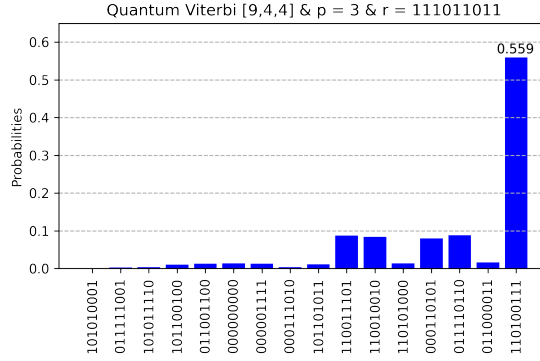


Figure 13: Solution corresponding to a $[9, 4, 4]$ code, found using UPO. We label the states with convention that the most significant bit is at the bottom. UPO uses $p = 3$, $q = 5$. The decoder estimates the path 111001011 having minimum path metric corresponding to received $r = 111011011$. The path metric is $d(111001011, r) = 1$.

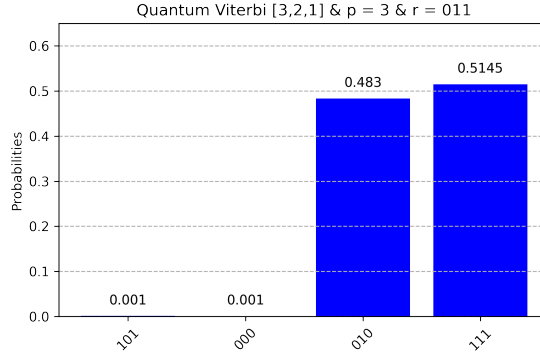


Figure 14: Solution corresponding to a $[3, 2, 1]$ code, found using UPO. We label the states with convention that the most significant bit is at the bottom. The codespace is $\mathcal{C} = \{000, 010, 101, 111\}$. UPO uses $p = 3$, $q = 5$. The decoder estimates two paths having the least path metric corresponding to the received $r = 011$. The path metric is $d(010, r) = d(111, r) = 1$.

6 Application to Convolution Codes

We apply the Viterbi decoder we constructed using the methods in Section 4 and 5 for decoding convolution codes. We use the rate $\frac{1}{2}$ code, with the number of message bits $k = 1$, the number of output codeword bits $n = 2$ at each time instant of the encoder. The

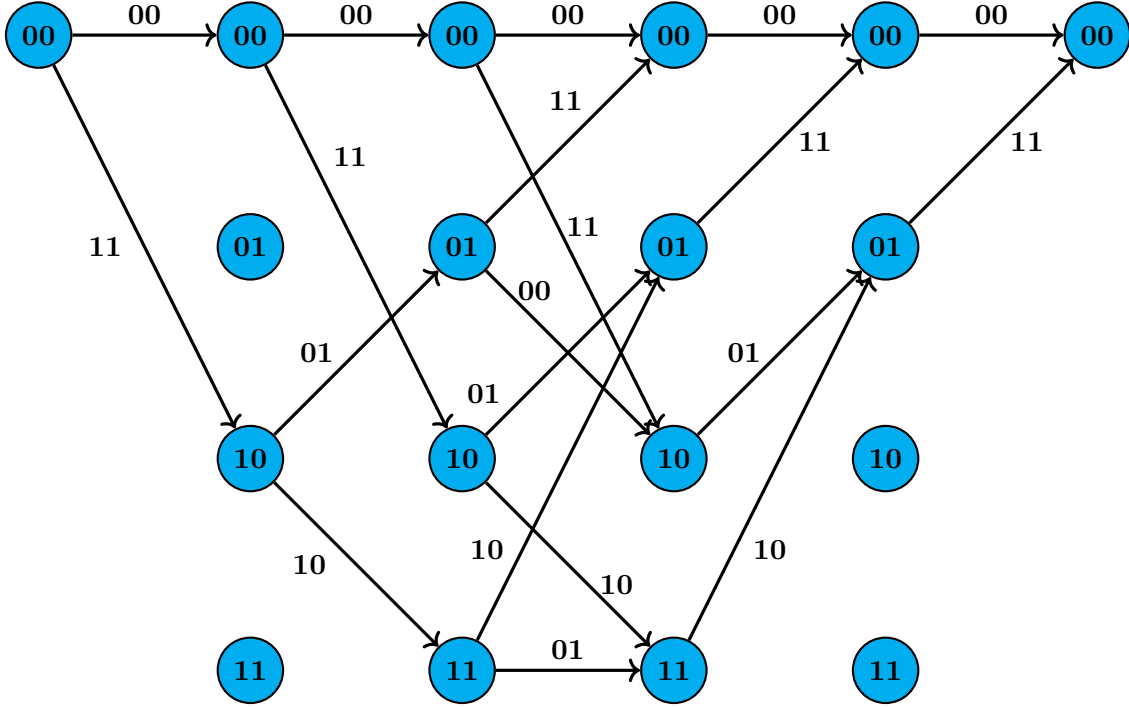
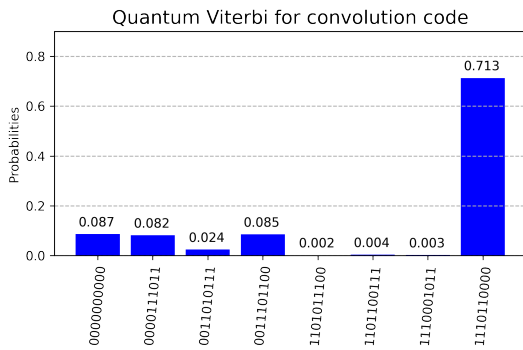
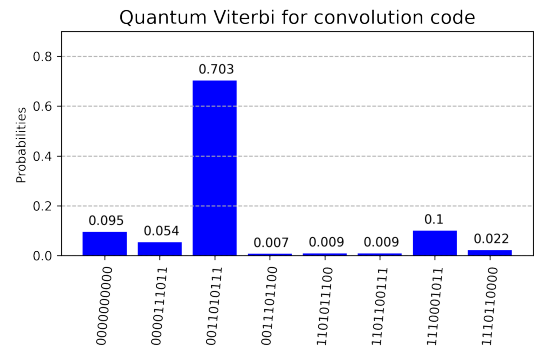


Figure 15: Trellis of the rate $\frac{1}{2}$ convolution encoder [18]. Between initial and final state there are 5 time instants. At each instant the input to the encoder is either 0 or 1. The branches are labeled according to the 2 bit output at each time instant. There are two branches from each node due to two possible input at each instant.

number of shift registers present in the encoder is $m = 2$. We let the encoder run for 5 time instances, so, the codeword has a total of 10 bits. At each time instant t , the input bit is defined as u_t . Then the state of the encoder we define as $S_t = (u_{t-1} u_{t-2})$, where u_{t-1} and u_{t-2} are the input bits at time instants $t - 1$ and $t - 2$ respectively. The trellis of this rate $\frac{1}{2}$ encoder [18] is shown in Fig. 15. The quantum Viterbi decoder uses UPO,



(a) Initial state is $|0000000000\rangle$. The received erroneous vector is $r = 0001110111$. Hamming distance between simulation output state and r is 1.



(b) Initial state is $|1101110000\rangle$. The received erroneous vector is $r = 1110001100$. Hamming distance between simulation output state and r is 1.

Figure 16: We show the results of the quantum Viterbi decoder for a rate $\frac{1}{2}$ convolution code, with $k = 1, n = 2, m = 2$, where m is the number of memory elements. We label different states along the horizontal axis, with the convention that the most significant bit is at the bottom. The number of QAOA unitary layers applied is $p = 3$. In Fig. 16a we start with a valid initial state $|0\rangle^{\otimes 10}$. In Fig. 16b the initial state is $|1101110000\rangle$.

mentioned in Algorithm 1. The cost unitary is exactly the same as in Eq. 33. We note that n , the total number of codeword bits, is 10. The mixer Hamiltonian is constructed using the Theorem 1. The codespace \mathcal{C} has 8 members, corresponding to 8 valid paths shown in the trellis Fig. 15. The codespace is

$$\mathcal{C} = \{0000000000, 0000110111, 0011011100, 0011101011, \\ 1101110000, 1101000111, 1110101100, 1110011011\}.$$

The minimum Hamming weight of the code is $d = 5$. Using Theorem 1, we state the mixer Hamiltonian is

$$H_m = X_1X_2X_4X_5X_6 + X_3X_4X_6X_7X_8 + X_5X_6X_8X_9X_{10}. \quad (40)$$

The corresponding mixer unitary is $U_m = e^{-i\beta H_m}$, where H_m is used from Eq. 40. We have shown the result of simulations in Fig. 16 for different received vectors to determine the least paths on the trellis shown in Fig. 15. The results of Fig. 16 show the feasibility and flexibility of the algorithm for different classical codes.

7 Conclusion and future research

We proposed a Quantum Approximation Optimization algorithm, which uses parameters uniformly optimized for the mixer and cost unitaries in the PQC. We showed through simulation that taking the parameters uniformly helps better optimization than taking them non-uniformly. We used this variational approach to construct a hybrid Viterbi decoder. We observed that the constructed hybrid decoder opts out any number of shortest paths present in the trellis as a solution. This quantum-classical decoder shares the workload and it even works well for shallow unitary depths. We showed that the structure of the unitaries depends on the type of classical error-correcting code. Thus, the algorithm can generally be implemented in NISQ devices with quantum error-correcting codes.

We point out some future works that can be extended on this. Finding the shortest path using a variational approach can be extended beyond classical encoding-decoding problems. Inference problems can also be approached using the method we adopted. One can design a unitary to produce an equal superposition of all the possible solutions. Depending on the history of the system, one can try to minimize certain path metrics related to the problem to suggest a suitable solution. Also, for search problems although Grover's search is optimal, this algorithm might be an alternative in terms of circuit depth. The quantum-classical hybrid approach will generally require low-depth quantum circuits compared to Grover's search.

References

- [1] Eric R Anschuetz and Bobak T Kiani. Quantum variational algorithms are swamped with traps. *Nature Communications*, 13(1):7760, 2022. DOI: <https://doi.org/10.1038/s41467-022-35364-5>.
- [2] Lalit Bahl, John Cocke, Frederick Jelinek, and Josef Raviv. Optimal decoding of linear codes for minimizing symbol error rate (corresp.). *IEEE Transactions on information theory*, 20(2):284–287, 1974. DOI: <https://doi.org/10.1109/TIT.1974.1055186>.
- [3] Elwyn Berlekamp, Robert McEliece, and Henk Van Tilborg. On the inherent intractability of certain coding problems (corresp.). *IEEE Transactions on Information Theory*, 24(3):384–386, 1978. DOI: <https://doi.org/10.1109/TIT.1978.1055873>.

- [4] Ethan Bernstein and Umesh Vazirani. Quantum complexity theory. In *Proceedings of the twenty-fifth annual ACM symposium on Theory of computing*, pages 11–20, 1993. DOI: <https://doi.org/10.1145/167088.167097>.
- [5] Mainak Bhattacharyya and Ankur Raina. A quantum algorithm for syndrome decoding of classical error-correcting linear block codes. In *2022 IEEE/ACM 7th Symposium on Edge Computing (SEC)*, pages 456–461. IEEE, 2022. DOI: <https://doi.org/10.1109/SEC54971.2022.00069>.
- [6] Lennart Bittel and Martin Kliesch. Training variational quantum algorithms is np-hard. *Physical review letters*, 127(12):120502, 2021. DOI: <https://doi.org/10.1103/PhysRevLett.127.120502>.
- [7] Jehoshua Bruck and Moni Naor. The hardness of decoding linear codes with preprocessing. *IEEE Transactions on Information Theory*, 36(2):381–385, 1990. DOI: <https://doi.org/10.1109/18.52484>.
- [8] Marco Cerezo, Akira Sone, Tyler Volkoff, Lukasz Cincio, and Patrick J Coles. Cost function dependent barren plateaus in shallow parametrized quantum circuits. *Nature communications*, 12(1):1791, 2021. DOI: <https://doi.org/10.1038/s41467-021-21728-w>.
- [9] David Deutsch and Richard Jozsa. Rapid solution of problems by quantum computation. *Proceedings of the Royal Society of London. Series A: Mathematical and Physical Sciences*, 439(1907):553–558, 1992. DOI: <https://doi.org/10.1098/rspa.1992.0167>.
- [10] Christoph Durr and Peter Hoyer. A quantum algorithm for finding the minimum. *arXiv preprint quant-ph/9607014*, 1996. DOI: <https://doi.org/10.48550/arXiv.quant-ph/9607014>.
- [11] Edward Farhi, Jeffrey Goldstone, and Sam Gutmann. A quantum approximate optimization algorithm. *arXiv preprint arXiv:1411.4028*, 2014. DOI: <https://doi.org/10.48550/arXiv.1411.4028>.
- [12] G David Forney. The viterbi algorithm. *Proceedings of the IEEE*, 61(3):268–278, 1973. DOI: <https://doi.org/10.1109/PROC.1973.9030>.
- [13] Jon R Grice and David A Meyer. A quantum algorithm for viterbi decoding of classical convolutional codes. *Quantum Information Processing*, 14(7):2307–2321, 2015. DOI: <https://doi.org/10.1007/s11128-015-1003-3>.
- [14] Lov K Grover. A fast quantum mechanical algorithm for database search. In *Proceedings of the twenty-eighth annual ACM symposium on Theory of computing*, pages 212–219, 1996. DOI: <https://doi.org/10.1145/237814.237866>.
- [15] Stuart Hadfield. On the representation of boolean and real functions as hamiltonians for quantum computing. *ACM Transactions on Quantum Computing*, 2(4):1–21, 2021. DOI: <https://doi.org/10.1145/3478519>.
- [16] Hyunwoo Jung, Jeonghwan Kang, and Jeongseok Ha. Quantum maximum likelihood decoding for linear block codes. In *2020 International Conference on Information and Communication Technology Convergence (ICTC)*, pages 227–232. IEEE, 2020. DOI: <https://doi.org/10.1109/ICTC49870.2020.9289350>.
- [17] Xinwei Lee, Yoshiyuki Saito, Dongsheng Cai, and Nobuyoshi Asai. Parameters fixing strategy for quantum approximate optimization algorithm. In *2021 IEEE international conference on quantum computing and engineering (QCE)*, pages 10–16. IEEE, 2021. DOI: <https://doi.org/10.1109/QCE52317.2021.00016>.
- [18] Shu Lin and Daniel J. Costello. *Error Control Coding, Second Edition*. Prentice-Hall, Inc., USA, 2004. ISBN 0130426725.
- [19] Jarrod R McClean, Sergio Boixo, Vadim N Smelyanskiy, Ryan Babbush, and Hartmut

- Neven. Barren plateaus in quantum neural network training landscapes. *Nature communications*, 9(1):4812, 2018. DOI: <https://doi.org/10.1038/s41467-018-07090-4>.
- [20] John Preskill. Quantum computing in the nisq era and beyond. *Quantum*, 2:79, 2018. DOI: <https://doi.org/10.22331/q-2018-08-06-79>.
- [21] Yue Ruan, Samuel Marsh, Xilin Xue, Zhihao Liu, Jingbo Wang, et al. The quantum approximate algorithm for solving traveling salesman problem. *Computers, Materials & Continua*, 63(3):1237–1247, 2020. DOI: <https://doi.org/10.32604/cmc.2020.010001>.
- [22] Daniel R Simon. On the power of quantum computation. *SIAM journal on computing*, 26(5):1474–1483, 1997. DOI: <https://doi.org/10.1137/S0097539796298637>.
- [23] Andrew Viterbi. Error bounds for convolutional codes and an asymptotically optimum decoding algorithm. *IEEE transactions on Information Theory*, 13(2):260–269, 1967. DOI: <https://doi.org/10.1109/TIT.1967.1054010>.

A Appendix

A.1 Mapping of a Hermitian and it's time evolution unitary

We elaborate one of the steps we used to proof Theorem 1. In Eq. 25, we implied

$$\begin{aligned} &\implies e^{-i\beta H_m} |\psi_{in}\rangle \in \mathcal{C}, \\ &\implies H_m |\psi_{in}\rangle \in \mathcal{C}. \end{aligned}$$

Now as H_f and H_m are non commuting $|\psi_{in}\rangle$ is not an eigenstate of H_m . But as the eigenstates of the hermitian H_m forms a basis, $|\psi_{in}\rangle$ can be expressed as a linear combination of them.

$$|\psi_{in}\rangle = \sum_{i=1}^n a_i |E_m\rangle_i, \quad (41)$$

where $|E_m\rangle_i$ are the eigenstates of H_m and a_i are the coefficients. Also $|\psi_{in}\rangle \in \mathcal{C}$. Now the operator $U_m = e^{-i\beta H_m}$ essentially is the time evolution operator, with β as the time parameter. We can express the state after the operation of U_m as:

$$\begin{aligned} \psi(\beta) &= U_m |\psi_{in}\rangle, \\ &= e^{-i\beta H_m} |\psi_{in}\rangle. \end{aligned} \quad (42)$$

Any exponential of a matrix can be expressed as a power series expansion,

$$e^{-i\beta H_m} = \mathbf{I} - i\beta H_m - \frac{\beta^2}{2!} H_m^2 + \dots \quad (43)$$

This power series converges for certain power of the Hamiltonian. Now as $|\psi_{in}\rangle$ is not an eigenstate of H_m . Eq. 42 can not be expressed in a closed form. But $|E_m\rangle_i$ are eigenstates of the Hamiltonian H_m thus,

$$\begin{aligned} U_m |E_m\rangle_i &= e^{-i\beta H_m} |E_m\rangle_i, \\ &= (\mathbf{I} - i\beta H_m - \frac{\beta^2}{2!} H_m^2 + \dots) |E_m\rangle_i, \\ &= (\mathbf{I} - i\beta E_{mi} - \frac{\beta^2}{2!} E_{mi}^2 + \dots) |E_m\rangle_i, \\ &= e^{-i\beta E_{mi}} |E_m\rangle_i, \end{aligned} \quad (44)$$

where E_{mi} is the eigenvalue of H_m corresponding to the eigenstate $|E_m\rangle_i$. Now we can use all these tools to show why both the time evolution unitary and the corresponding hermitian has the same mapping. According to Theorem 1, $H_m|\psi_{in}\rangle \in \mathcal{C}$. As the codespace of linear block code is linear, following Eq. 41 it is obvious that $E_{mi} \in \mathcal{C}$. Now using Eq. 44 and completeness of the eigenstates of H_m in Eq. 42, we have

$$\begin{aligned}\psi(\beta) &= e^{-i\beta H_m} |\psi_{in}\rangle, \\ &= \sum_i e^{-i\beta H_m} |E_m\rangle_i \langle E_m|_i |\psi_{in}\rangle, \\ &= \sum_i e^{-i\beta E_{mi}} |E_m\rangle_i \langle E_m|_i |\psi_{in}\rangle, \\ &= \sum_i a_i e^{-i\beta E_{mi}} |E_m\rangle_i.\end{aligned}\tag{45}$$

Eq. 45 proves that $\psi(\beta) \in \mathcal{C}$. Expressing the initial state as a superposition of the eigenstates H_m only adds phases into the corresponding terms in the superposition when U_m is applied to it. Thus, the unitary U_m and the Hamiltonian H_m have the same mapping on states.

A.2 Circuit of the mixer for the [6,3,3] code

The mixer for the [6,3,3] linear block code is defined as $U_m(\beta) = e^{-i\beta H_m}$. $U_m(\beta)$ is expressed in Eq. 35. We show the circuit diagram of the mixer below.

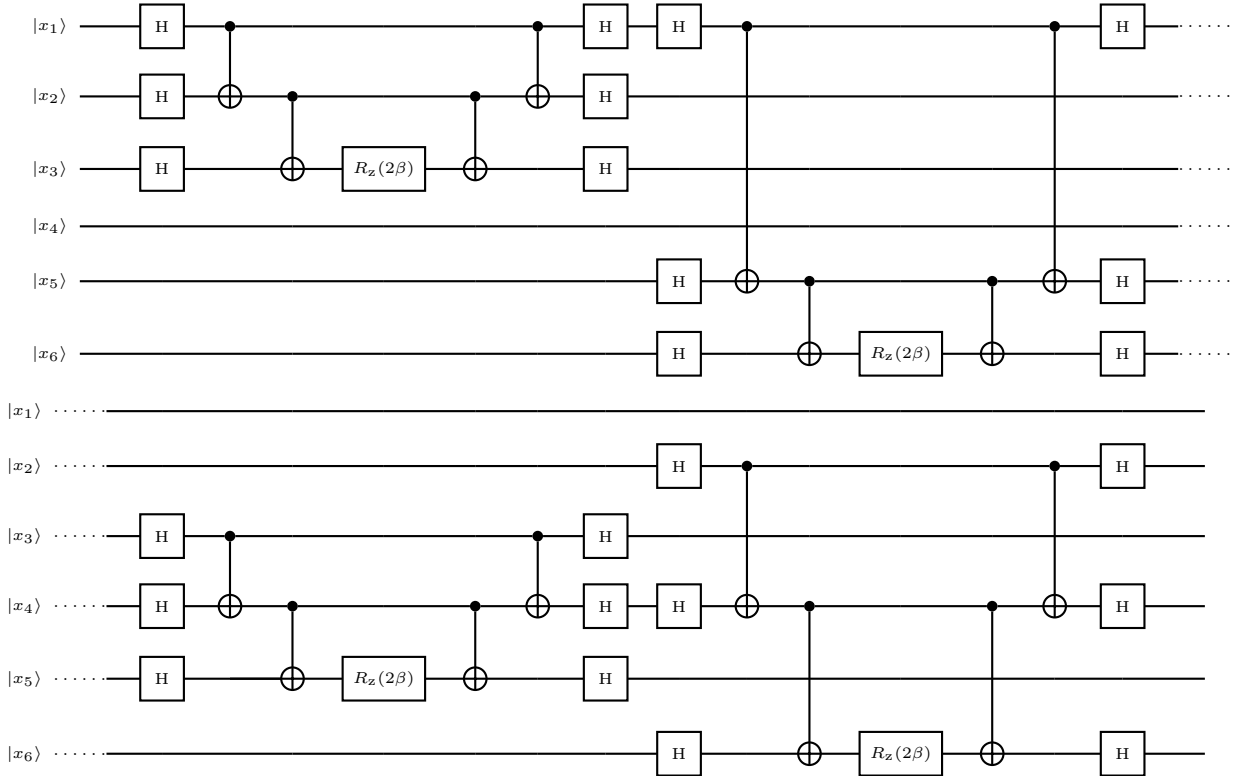


Figure 17: Mixer $U_m(\beta)$ for the [6,3,3] linear block code. We exclude the ancilla register for showing the mixer circuit as they have no part in it. Horizontal dots are used to represent the circuit continuation. $R_z(-\gamma)$ is the single qubit rotation gate about the z axis, $R_z(2\beta) = e^{-i\beta Z}$.

A.3 Circuit of the cost unitary for the $[6,3,3]$ code

Here we show the detail circuit of how we implement the cost unitary $U_f(\gamma)$. The cost unitary for the $[6,3,3]$ code is defined in Eq.33. In Fig.18, the connection between the codeword register x and the ancilla register r is shown.

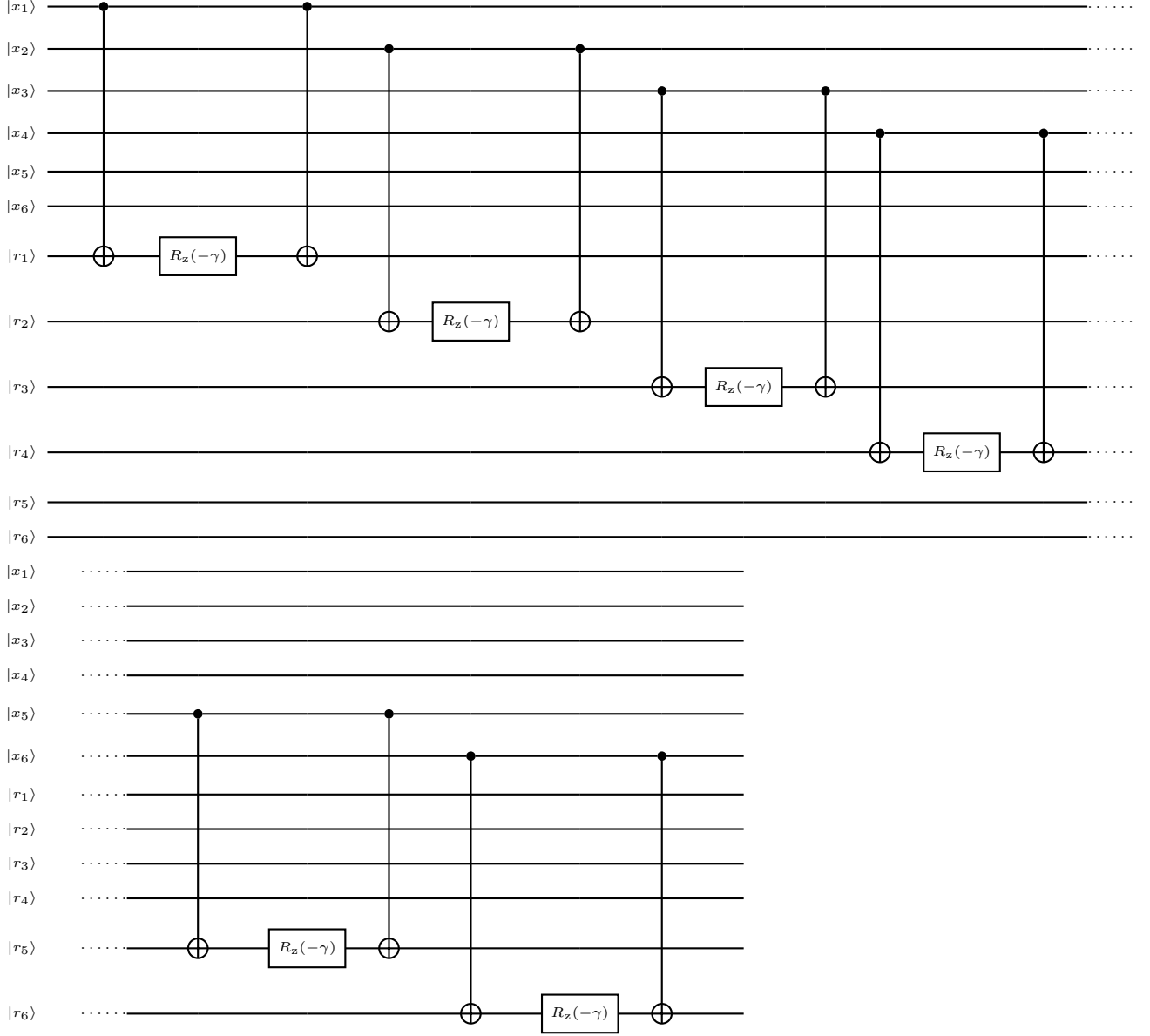


Figure 18: Cost unitary $U_f(\gamma)$ for the $[6,3,3]$ linear block code. Horizontal dots are used to represent the circuit continuation. $R_z(-\gamma)$ is the single qubit rotation gate about the z axis, $R_z(-\gamma) = e^{i\frac{\gamma}{2}Z}$.